Rapid blood acid-base regulation by European sea bass (*Dicentrarchus labrax*) in response to sudden exposure to high environmental CO_2

Running title: Rapid acid-base regulation by bass

Daniel W. Montgomery[a*], Garfield T. Kwan[b,c], William G. Davison[a], Jennifer Finlay[a], Alex Berry[a], Stephen D. Simpson[a], Georg H. Engelhard[d,e], Silvana N.R. Birchenough[b], Martin Tresguerres[b], Rod W. Wilson[a*]

[a] Biosciences, Geoffrey Pope Building, University of Exeter, UK

[b] Marine Biology Research Division, Scripps Institution of Oceanography, University of California San Diego, 9500 Gilman Drive, La Jolla, CA, 92093, USA

[c] National Oceanic and Atmospheric Administration Fisheries Service, Southwest Fisheries Science Center, 8901 La Jolla Shores Drive, La Jolla, CA, 92037, USA

[d] Centre for Environment, Fisheries & Aquaculture Science (Cefas), Pakefield Road, Lowestoft, UK

[e] School of Environmental Sciences, University of East Anglia, Norwich, UK

[*]corresponding authors: danwmont@gmail.com/R.W.Wilson@exeter.ac.uk

Summary statement: European sea bass exposed to 1 kPa (10,000 µatm) CO_2 regulate blood and red cell pH within 2 hours and 40 minutes, respectively, protecting O_2 transport capacity, via enhanced gill acid excretion.

Keywords: hypercapnia, ionocytes, respiratory acidosis, O_2 transport, gill plasticity

Abstract

Fish in coastal ecosystems can be exposed to acute variations in CO_2 that can approach 1 kPa CO_2 (10,000 µatm). Coping with this environmental challenge will depend on the ability to rapidly compensate the internal acid-base disturbance caused by sudden exposure to high environmental CO_2 (blood and tissue acidosis); however, studies about the speed of acid-base regulatory responses in marine fish are scarce. We observed that upon exposure to ~1 kPa CO_2, European sea bass (*Dicentrarchus labrax*) completely regulate erythrocyte intracellular pH within ~40 minutes, thus restoring haemoglobin-O_2 affinity to pre-exposure levels. Moreover, blood pH returned to normal levels within ~2 hours, which is one of the fastest acid-base recoveries documented in any fish. This was achieved via a large upregulation of net acid excretion and accumulation of HCO_3^- in blood, which increased from ~4 to ~22 mM. While the abundance and intracellular localisation of gill Na^+/K^+-ATPase (NKA) and Na^+/H^+ exchanger 3 (NHE3) remained unchanged, the apical surface area of acid-excreting gill ionocytes doubled. This constitutes a novel mechanism for rapidly increasing acid excretion during sudden blood acidosis. Rapid acid-base regulation was completely prevented when the same high CO_2 exposure occurred in seawater with experimentally reduced HCO_3^- and pH, likely because reduced environmental pH inhibited gill H^+ excretion via NHE3. The rapid and robust acid-base regulatory responses identified will enable European sea bass to maintain physiological performance during large and sudden CO_2 fluctuations that naturally occur in coastal environments.

Introduction

Increased CO_2 in aquatic environments, or environmental hypercapnia, causes significant physiological challenges for water breathing animals including fish. As environmental CO_2 increases, there is a corresponding rise in CO_2 within the fish's blood, which in turn induces a decrease in blood pH. This condition is referred to as a respiratory acidosis, and depending on its magnitude, can disrupt multiple homeostatic processes including gas exchange (Crocker and Cech Jr, 1998; Eddy et al., 1977; Perry and Kinkead, 1989) and cardiovascular function (Lee et al., 2003; Perry and McKendry, 2001; Perry et al., 1999). Globally, CO_2

levels in the ocean are increasing as a result of anthropogenic climate change, and are predicted to reach ~0.1 kPa (0.1% CO_2, 1,000 µatm) by 2100 under a 'business as usual' scenario (Orr et al., 2005; Doney et al., 2011; IPCC, 2014).

The increase in oceanic CO_2 levels, known as ocean acidification (OA) (Doney et al., 2009), has renewed interest in acid-base regulatory mechanisms of aquatic organisms. However, coastal and estuarine environments already experience much larger variations in CO_2 levels (Sunda and Cai, 2012; Wallace et al., 2014), which will likely be exacerbated in the future (Cai et al., 2011; Melzner et al., 2013). These fluctuations may occur rapidly over minutes to hours, and reach levels as high as ~1 kPa (1% CO_2, 10,000 µatm) (Borges *et al.*, 2006; Baumann *et al.*, 2015). This type of environmental hypercapnia implies a different physiological challenge compared to OA. Firstly, as environmental CO_2 levels increase above CO_2 levels in venous blood (typically ~0.3 kPa), CO_2 diffusion gradients are reversed resulting in net uptake from the environment into the blood and inducing a much more pronounced respiratory acidosis (Tresguerres and Hamilton, 2017). Secondly, the sudden and extreme CO_2 fluctuations must be met by equally fast, robust, and reversible acid-base regulatory responses.

Fish have a great capacity to restore blood pH to compensate for CO_2-induced respiratory acidosis, which is largely achieved by excreting excess H^+ and absorbing HCO_3^- using their gills (Brauner et al., 2019; Claiborne et al., 2002; Esbaugh, 2017; Evans et al., 2005; Perry and Gilmour, 2006). At the cellular level, these processes take place in specialized ion-transporting cells, or ionocytes. However, the underlying ion-transporting proteins and regulatory mechanisms are intrinsically different between freshwater and marine fishes and may also vary between species (Brauner and Baker, 2009; Claiborne et al., 2002; Evans et al., 2005; Perry and Gilmour, 2006). The few studies that have investigated acid-base regulation after acute exposure to ~1 kPa CO_2 in marine fish have reported large variation of responses, with full blood pH compensation occurring between ~2 and 24 hours depending on the species (Hayashi et al., 2004; Larsen et al., 1997; Perry, 1982; Toews et al., 1983). Given the exquisite sensitivity of most proteins to changes in pH, variation in the time course of acid-base regulatory responses between species has important implications for whole organism performance. Haemoglobins (Hb) of fish species show strong Bohr and Root effects (Wells, 2009) which reduces Hb-O_2 binding affinity and the O_2 carrying

capacity when erythrocyte intracellular pH (pH_i) decreases. While fish have adaptations to regulate pH_i of erythrocytes (Cossins and Richardson, 1985; Nikinmaa and Tufts, 1989; Thomas and Perry, 1992), erythrocyte pH_i in many fish species (particularly marine fish) is closely linked to whole blood pH (Brauner and Baker, 2009; Shartau et al., 2020). Therefore, adaptations which enhance the speed of whole blood acid-base regulation will also provide faster restoration of O_2 transport capacity and minimise disruption to energetically expensive activities such as foraging and digestion. However, little is known about why some species are able to compensate respiratory acidosis faster than others.

The gill ionocytes of marine fish excrete H^+ using apical Na^+-H^+ exchangers (NHEs) driven by basolateral Na^+/K^+-ATPase (NKAs) (Brauner et al., 2019; Claiborne et al., 2002; Evans et al., 2005). Theoretically, H^+ excretion during sudden exposure to hypercapnia could be upregulated by increased biosynthesis of NKA and NHE; however, transcriptional and translational responses typically take at least a few hours (e.g. Tresguerres *et al.*, 2005, 2006). Furthermore, protein turnover is energetically expensive (Pan et al., 2015), so short-term regulation of H^+ excretion by synthesis and degradation of ion-transporting proteins would not be particularly efficient. Alternatively, the rapid upregulation of H^+ excretion may be mediated by post-translational regulatory modifications such as insertion of pre-existing proteins into the ionocyte membrane, or morphological adjustments of its apical area, as reported by a variety of fishes in response to other acid-base disturbances (reviewed in Brauner et al., 2019; Tresguerres et al., 2019).

In the present study we investigated acid-base regulation of European sea bass, *Dicentrarchus labrax*, an active predator which seasonally inhabits shallow coastal, estuarine and saltmarsh environments (Doyle et al., 2017) where rapid and large fluctuations in CO_2 levels occur (Borges et al., 2006). Specifically, we characterised blood acid-base regulation, erythrocyte intracellular pH (pH_i) and O_2 affinity, effects of seawater chemistry on speed of acid-base regulation, and changes in ionocyte NKA and NHE3 abundance, intracellular localisation, and apical surface area during acute exposure to ~1 kPa CO_2.

Methods

Capture and Pre-Experimental Condition

Juvenile European sea bass were obtained by seine netting in estuaries and salt marshes from Dorset and the Isle of Wight on the south coast of the United Kingdom. Sea bass were transferred to the Aquatic Resources Centre of the University of Exeter where they were held in ~500 L tanks in a recirculating aquaculture system (RAS, total volume ~ 2500 L) at temperatures between 14 and 22°C. Sea bass were fed three times a week with commercial pellet (Horizon 80, Skretting) with a supplement of chopped frozen mussel (*Mytilus* edulis) once a week. For ~6 months before experiments sea bass were maintained at a temperature of 14°C and seawater CO_2 levels of ~0.05-0.06 kPa (pH~8.10). Prior to all experimental procedures, sea bass were withheld food for a minimum of 72 hours. Animal collections were conducted under appropriate permits (Marine Management Organisation permit #030/17 & Natural England permit #OLD1002654) and all experimental procedures were carried out under home office licence P88687E07 and approved by the University of Exeter's Animal Welfare and Ethical Review Board.

Hypercapnia exposure

Individual sea bass were moved to isolation tanks (~20 L) and left to acclimate overnight for a minimum of 12 hours before exposure to hypercapnia. During the acclimation period isolation tanks were fed by the RAS at a rate of ~4 L min^{-1}; with overflowing water recirculated back to the RAS. After overnight acclimation, hypercapnia exposure began by switching inflow of water from low CO_2 control conditions to high CO_2 seawater delivered from a header tank (~150 L) in which pCO_2 levels had already been increased to ~1 kPa using an Aqua Medic pH computer (AB Aqua Medic GmbH). The pH computer maintained header tank pCO_2 levels using an electronic solenoid valve which fed CO_2 to a diffuser in the header tank if pH rose above 6.92 and stopped CO_2 flow if pH dropped below 6.88. Additionally, to reduce CO_2 fluctuation in isolation tanks during exposures, the gas aerating each tank was switched from ambient air to a gas mix of 1% CO_2, 21% O_2 and 78% N_2 (G400 Gas mixing system, Qubit Biology Inc.). During exposures overflowing water from each isolation tank recirculated to the header tank creating an isolated experimental system of ~250 L. The experimental system was maintained at 14°C using a heater/chiller unit (Grant TX150 R2, Grant Instruments) attached to a temperature exchange coil in the header tank. To characterise the time course of acid-base regulation sea bass were exposed

to hypercapnia (~1 kPa CO_2) for either ~10 minutes, ~40 minutes, or ~135 minutes before measurements were taken. pH of isolation tanks was monitored with a separate pH probe and matched the header tank ~5 minutes after initial exposure. Measurements of an additional group of sea bass were obtained at normocapnic CO_2 levels (~0.05 kPa CO_2) to act as a pre-exposure control (hereafter this group is referred to as time = 0). At the time of sampling measurements of seawater pH (NBS scale), temperature and salinity, as well as samples of seawater to measure total CO_2 (TCO_2)/Dissolved Inorganic Carbon (DIC), were taken from each isolation tank. DIC analysis was conducted using a custom built system described in detail by Lewis *et al.* (2013). Measurements of pH, salinity, temperature and DIC were then input into CO2SYS (Pierrot et al., 2006) to calculate *p*CO2 and total alkalinity (TA) based on the equilibration constants refitted by Dickson and Millero (1987).

Blood sampling and analysis

Following hypercapnia exposures (Table 1), sea bass were individually anaesthetised in-situ with a dose of 100 mg L^{-1} benzocaine. Blood samples were then obtained following the methodology outlined by Montgomery *et al.* (2019). The gill irrigation tank used was filled with water from the header tank and maintained at an appropriate CO_2 level by aeration with the same gas mix feeding the isolation tanks. The water chemistry of the gill irrigation chamber was measured following the same procedures outlined for the isolation chambers, with one DIC sample taken at the end of blood sampling (Table S1).

Table 1: Mean ± s.e.m. of water chemistry parameters within isolation tanks during hypercapnia exposures prior to blood sampling.

	Duration			
	0 min (Control)	~10 min (10.8 ± 0.26 min)	~40 min (41.0 ± 2.82 min)	~135 min (133.9 ± 2.27 min)
Temperature (°C)	13.94 ± 0.04	13.90 ± 0.03	13.94 ± 0.02	13.89 ± 0.04
pH (NBS)	8.15 ± 0.01	6.98 ± 0.01	6.96 ± 0.01	6.95 ± 0.01
Salinity	34.1 ± 0.1	34.1 ± 0.1	34.7 ± 0.2	34.0 ± 0.1
***p*CO_2 (kPa)**	0.059 ± 0.001	0.898 ± 0.022	0.944 ± 0.072	0.945 ± 0.017
TA (µM)	3,251 ± 20	2,804 ± 16	2,833 ± 11	2,777 ± 29

Immediately after sampling, extracellular pH was measured on 30 µL of whole blood using an Accumet micro pH electrode and Hanna HI8314 pH meter calibrated to 14 °C using pH_{NBS} 7.04 and 9.21 appropriate buffers. Measurements of blood pH were made in a temperature-controlled water bath. Three 75 µL micro capillary tubes were then filled with whole blood and anaerobically sealed with Critoseal capillary tube sealant (Fisher) and paraffin oil and centrifuged for 2 minutes at 10,000 rpm. Haematocrit (Hct) was measured using a Hawksley micro-haematocrit reader. Plasma was then extracted from capillary tubes for analysis of TCO_2 using a Mettler Toledo 965D carbon dioxide analyser. Plasma pCO_2 and HCO_3^- were then calculated from TCO_2, temperature and blood pH using the Henderson-Hasselbalch equation with values for solubility and pK^1_{app} based on Boutilier *et al.* (1984, 1985). Haemoglobin (Hb) content of 10 µL of whole blood was also assessed by the cyanmethemoglobin method (after addition to 2.5 mL of Drabkin's reagent, Sigma). Half the remaining whole blood was centrifuged at 10,000 rpm for 2 minutes at 4°C. The resulting plasma was separated and 10 µL was diluted in ultrapure water, snap frozen in liquid N_2, and stored at -80°C before later being used to measure plasma cation and anion concentrations using ion chromatography (Dionex ICS 1000 & 1100, Thermo-Scientific, UK). The remaining plasma was snap frozen in liquid N_2 and stored at -80°C before measurements of plasma lactate and glucose were made (YSI 2900D Biochemistry Analyzer, Xylem Analytics). After separating the plasma, the surface of the leftover erythrocyte pellet was blotted to remove the leukocyte layer. The erythrocyte pellet was then snap frozen in liquid nitrogen for 10 seconds and thawed in a 37°C water bath for 1 minute prior to intracellular pH (pH_i) measurements as described by Zeidler and Kim (1977), and validated by Baker *et al.* (2009). All measurements or storage of blood occurred within 10 minutes of blood sampling. Finally, Hb-O_2 affinity was measured following the methods outlined in Montgomery *et* al. (2019) using a Blood Oxygen Binding System (BOBS, Loligo systems), as detailed by Oellermann *et al.* (2014).

Flux measurements

The flux of acid-base relevant ions between sea bass and seawater was measured over a ~135 minute time period in normocapnic conditions (n = 7) and immediately following exposure to hypercapnia (n = 8, Table 2). At the start of the measurements the flow to the isolation tanks was stopped and water

chemistry maintained at the desired pCO_2 by gassing the tanks with either ambient air (control) or a 1% CO_2 gas mix (hypercapnia). Seawater samples for measuring TA were taken at the beginning and end of the ~135 minute flux period, preserved by adding 40 µL of 4% (w/v) mercuric chloride per 10 mL of seawater, and stored at 4 °C (Dickson et al., 2007) prior to analysis by double titration using an autotitrator (Metrohm 907 Titrando with 815 Robotic USB Sample Processor XL, Metrohm). TA measurements were made using a double titration method modified from Cooper *et al.* (2010) as detailed by Middlemiss *et al.* (2016). Briefly, 20 mL samples were titrated to pH 3.89 using 0.02 M HCl whilst gassing with CO_2-free N_2, pH was then returned to starting values by titrating with 0.02 M NaOH. Samples for measuring total ammonia were frozen at -20°C before ammonia concentration was measured using a modified version of the colourimetric method of Verdouw *et al.* (1978) at 660 nm using a microplate reader (NanoQuant infinite M200 pro, Tecan Life Sciences). A calibration curve was constructed using NH_4Cl standards in seawater.

Table 2: Mean ± s.e.m. of water chemistry parameters within individual tanks during flux measurements.

Treatment	Duration (min)	pH (NBS)	Temperature (ºC)	Salinity	pCO_2 (kPa)	TA (µM)
Normocapnia	132.3 ± 0.9	7.96 ± 0.01	14.03 ± 0.04	33.6 ± 0.2	0.072 ± 0.002	2395 ± 21
Hypercapnia	123.6 ± 2.4	6.91 ± 0.03	13.90 ± 0.12	33.6 ± 0.0	0.862 ± 0.056	2299 ± 33

Acid-base relevant fluxes (µmol kg^{-1} h^{-1}) were then calculated using the following equation:

$$J_x = \left[\left([X]_i - [X]_f\right) \times V\right]/(M \times t)$$

as described by Wilson and Grosell (2003), where V is the volume of water (L) in the isolation tank (after the initial sample is taken), M is the mass of the sea bass (kg), t is the duration of the flux period (h) and $[X]_i$ and $[X]_f$ are the ion concentrations in the chamber water (µmol L^{-1}) at the beginning and end of the flux period. By reversing the initial and final values titratable acid, instead of base, fluxes can be calculated so that a positive value equals acid uptake (i.e. HCO_3^- excretion) and a negative value equals acid excretion (i.e. HCO_3^- uptake). We then calculated net acid-base fluxes (µeq kg^{-1} h^{-1}) as the sum of titratable acid and total ammonia (T_{amm}) flux (McDonald and Wood, 1981).

Exposure to Low Total Alkalinity

Sufficient 1 M HCl was added to ~250 L seawater to reduce TA by over 90% from ~2,800 µM to ~200 µM, followed by overnight aeration to equilibrate CO_2 with atmospheric levels. We then adjusted the pCO_2 of the low TA seawater to the desired level of ~1 kPa as described above, and a pH set point of 5.75. Sea bass were placed in the individual isolation boxes (fed by the RAS as detailed for normal TA hypercapnia exposures) and left to acclimate overnight before being exposed to the combined low TA and hypercapnia treatment. Flow to individual isolation boxes was stopped, and ~75% of the water from the isolation box was drained and refilled with low TA, hypercapnic water. This process was repeated 3 times over a period of ~5 minutes. The gas mix aerating each isolation box was switched from ambient air to a 1% CO_2 gas mix to maintain the desired pCO_2 levels. After ~135 minutes exposure, each seabass was anaesthetised and sampled for blood acid-base measurements as detailed previously. The water chemistry of isolation boxes (Table S2) and gill irrigation chambers (Table S3) was measured at the time of blood sampling.

Gill sampling

Gill tissue was sampled from sea bass exposed to ambient CO_2 conditions (n = 5) and to hypercapnia for ~135 minutes (n=5, taken immediately after the flux measurements) in normal TA seawater (Table S4). Mean water chemistry conditions during flux measurements (Table 2) and experienced by sea bass prior to gill sampling (Table S4) differ because gill samples were only collected from 5 of the 8 sea bass used for flux measurements. After euthanizing the sea bass in an anaesthetic bath (benzocaine, 1 g L^{-1}), gills were dissected and rinsed in phosphate buffered saline (PBS). The first gill arch on the left side was flash frozen in liquid N_2 and stored at -80°C for Western blotting, and the first gill arch on the right side was fixed in 4% paraformaldehyde in 0.1 M phosphate buffer saline (PBS) (diluted from 16% electron microscopy grade paraformaldehyde. Electron Microscope Science catalogue # 15710), overnight at 4°C for immunohistochemistry. Following a ~10-hour fixation, gill samples were transferred to 50% ethanol for ~10 hours at 4 °C, and then stored in 70% ethanol at 4°C.

Antibodies

NKA was immunodetected using α5, a mouse monoclonal antibody against the α-subunit of chicken NKA (a5, Developmental Studies Hybridoma Bank, Iowa City, IA, USA; Lebovitz *et al.*, 1989). This antibody universally recognizes NKA in teleost fishes including yellowfin tuna (*Thunnus albacares*; Kwan *et al.*, 2019), Pacific chub mackerel (*Scomber japonicus*; Kwan *et al.*, 2020), and California killifish (*Fundulus parvipinnis*; Nadler *et al.*, 2021). Rabbit anti-NHE3 polyclonal antibodies were generously donated by Dr Junya Hiroi (St. Marianna University School of Medicine, Kawaski, Japan); they target two epitope regions within rainbow trout (*Oncorhynchus mykiss*) NHE3b (GDEDFEFSEGDSASG and PSQRAQLRLPWTPSNLRRLAPL), and recognize NHE3 of multiple teleost species including European sea bass (*D. labrax*; Blondeau-Bidet *et al.*, 2019). The secondary antibodies were goat anti-mouse HRP-linked and goat anti-rabbit HRP-linked (Bio-Rad, Hercules, CA, USA) for immunoblotting, and goat anti-mouse Alexa Fluor 546 and goat anti-rabbit Alexa Fluor 488 (Invitrogen, Grand Island, USA) for immunohistochemistry.

Western Blotting

Western blotting followed the procedures outlined in Kwan *et al.*, (2019, 2020). While frozen on dry ice, the gill filament and lamellae were separated from the gill arch using a razor blade. The excised tissue was then immersed in liquid N_2 and pulverized in a porcelain grinder, then submerged within an ice-cold, protease inhibiting buffer (250 mmol L^{-1} sucrose, 1 mmol L^{-1} EDTA, 30 mmol L^{-1} Tris, 10 mmol L^{-1} benzamidine hydrochloride hydrate, 1 mmol L^{-1} phenylmethanesulfonyl fluoride, 1 mmol L^{-1} dithiothreitol, pH 7.5). Samples were further homogenized using a handheld VWR Pellet Mixer (VWR, Radnor, PA, USA) for 15 second intervals (3 times) while on ice. Next, samples were centrifuged (3,000 g, 4°C; 10 minutes), and the resulting supernatant was considered the crude homogenate. An aliquot of the crude homogenate was further subjected to a higher speed centrifugation (21,130xg, 4°C; 30 minutes), and the pellet was saved as the membrane-enriched fraction. Bradford assay was used to determine protein concentration (Bradford, 1976), which was used to normalize protein loading.

On the day of Western blotting, samples were mixed with an equal volume of 90% 2x Laemmli buffer and 10% β-mercaptoethanol. Samples were then heated at 70°C for 5 minutes, and the proteins (20 µg per lane) were loaded onto a

polyacrylamide mini gel (4% stacking; 10% separating) – alternating between control and high CO_2 treatments to avoid possible gel lane effects. The gel ran at 60 volts for 15 minutes, then 100 V for 1.5 hours, and proteins were transferred onto a polyvinylidene difluoride (PVDF) membrane using a wet transfer cell (Bio-Rad) at 70 volts for 2 hours at 4 °C. PVDF membranes were then incubated in Tris-buffered saline with 1% tween (TBS-T) with milk powder (0.1 g/mL) at room temperature for 1 hour, then incubated with primary antibody (NKA: 10.5 ng/ml; NHE3: 1:1,000) in blocking buffer at 4°C overnight. On the following day, PVDF membranes were washed in TBS-T (three times; 10 minutes each), incubated in blocking buffer with secondary antibodies (1:10,000) at room temperature for 1 hour, and washed again in TBS-T (three times; 10 minutes each). Bands were made visible through addition of ECL Prime Western Blotting Detection Reagent (GE Healthcare, Waukesha, WI) and imaged with the Universal III Hood (BioRad). Following imaging, the PVDF membrane was incubated in Ponceau stain (10 minutes, room temperature) to estimate protein loading. Relative NKA and NHE protein abundance (n = 5 per treatment) was quantified using the Image Lab software (version 6.0.1; BioRad) and normalized by the protein content in each lane.

Immunohistochemistry

Immunohistochemistry was performed as described in Kwan *et al.*, (2020). Fixed gill tissue stored in 70% ethanol was rehydrated in PBS + 0.1% tween (PBS-T) for 10 minutes, and gill filaments were dissected out to ease subsequent imaging. Autofluorescence was quenched by rinsing in ice-cold PBS with sodium borohydride (1.0 – 1.5 mg mL^{-1}; six times; 10 minutes each), followed by incubation in blocking buffer (PBS-T, 0.02% normal goat serum, 0.0002% keyhole limpet haemocyanin) at room temperature for one hour. Samples were incubated with blocking buffer containing primary antibodies (NKA: 40 ng/mL; NHE3: 1:500 [c.f. Seo *et al.*, (2013)]) at 4°C overnight. On the following day, samples were washed in PBS-T (three times at room temperature; 10 min each), and incubated with the fluorescent secondary antibodies (1:500) counterstained with DAPI (1 µg mL^{-1}) at room temperature for 1 hour. Samples were washed again in PBS-T as before, then placed on a concave slide for imaging using an inverted confocal microscope (Zeiss LSM 800 with Zeiss ZEN 2.6 blue edition

352 software; Cambridge, United Kingdom). Samples incubated without primary
353 antibodies had no signal (Fig. S1).

354 **Quantification of Ionocyte Apical Surface Area**

355 The apical surface area of gill ionocytes were quantified through a
356 combination of whole-mount imaging (40X objective lens with deionized water
357 immersion), optical sectioning, and XZ- and YZ-plane analysis. A relatively flat
358 surface on the gill filament was selected under 0.5x scanning confocal
359 magnification to ensure imaging would be performed on ionocytes in an upright
360 position thus minimizing errors in apical surface area quantification due to angle
361 distortion. After locating an ionocyte by its distinctive NKA signal, the scanning
362 confocal magnification was increased to 5.0X and the entire cell was Z-stack
363 imaged (optimal interval automatically selected: 0.07-0.12 µm per slice).
364 Subsequent viewing of the Z-stack from the X-Z and Y-Z planes allowed us to
365 assess intracellular localisation, and to identify the image slice that captured the
366 entire apical surface (typically, the second slice from the top of the cell). Next, the
367 ionocyte's apical surface area (identified by NHE3 immunofluorescence signal)
368 was quantified using FIJI (Schindelin et al., 2012). For each sea bass (n=5 per
369 treatment), the average apical surface area was calculated from three ionocytes
370 from different gill filaments.

371 **Statistical Analysis**

372 All statistical analysis was performed using R v3.6.3 (R Core Team, 2020).
373 Changes in blood chemistry parameters over time in response to hypercapnia
374 exposure were analysed using one-way ANOVA before assumptions of equal
375 variances of data and normality of model residuals were checked. Post-hoc tests
376 were conducted on least-square means generated by package 'emmeans'
377 (Lenth, 2020), with Tukey adjusted p-values for multiple comparisons. Some data
378 did not meet required assumptions for one-way ANOVA. Unequal variances were
379 observed in measurements of pCO_2 between treatments, as such we used
380 Welch's ANOVA with Tukey's pairwise comparisons using Benjamini-Hochberg
381 corrections for post-hoc testing. Measurements of blood pH and P_{50} did not meet
382 assumptions of normality and were analysed using the Kruskal-Wallis test with
383 post-hoc comparisons made with Dunn's test from package 'FSA' (Ogle et al.,
384 2020), using Benjamini-Hochberg corrections for multiple comparisons. As a
385 result of unusually high measurements of plasma [Cl^-] and [Na^+] in some samples

a ROUT test was conducted (Q = 0.5%) in Graphpad Prism 9 to identify potential outliers (Motulsky and Brown, 2006). Samples in which plasma [Cl^-] and [Na^+] were both identified as outliers by the ROUT test were excluded from the dataset prior to subsequent statistical analysis. Flux measurements were analysed using Student's t-test after checking data met assumptions of normality and equal variance. Relative protein abundance and ionocyte apical area met both assumptions of normality and equal variance and were analysed using one-tailed t-test (control response < CO_2-exposed response).

Results

Blood chemistry

Exposure to environmental hypercapnia caused significant changes in blood pH of sea bass over time (Kruskal-Wallis test, $\chi^2 = 25.0$, df = 3, $p < 0.001$). There was a pronounced acidosis of the blood from pH 7.84 (± 0.02) in control conditions (normocapnia, time = 0) to 7.50 (± 0.03) after exposure to hypercapnia for ~10 minutes (Fig. 1A, D). Following this initial acidosis sea bass completely restored blood pH to control levels after ~135 minutes (Fig. 1A, D). Blood pH regulation was accompanied by a ~5-fold increase in plasma HCO_3^-, from 4.5 ± 0.3 to 21.9 ± 0.7 mM, over the ~135 minute exposure (Fig. 1C, D, One-way ANOVA, F = 203.3, df = 3, $p < 0.001$).

Plasma pCO_2 showed significant changes during exposure to hypercapnia (Fig. 1B, D, Welch's ANOVA, F = 202.5, df = 3, $p < 0.001$). The initial decrease in blood pH of sea bass was driven by a rapid and large (~6-fold) increase in plasma pCO_2, from 0.200 ± 0.016 to 1.185 ± 0.049 kPa CO_2, within the first 10 minutes of exposure. There was a small but significant decline in plasma pCO_2 between sea bass sampled ~10 minutes after exposure and sea bass sampled ~135 minutes after exposure (Fig. 1B). There were no significant differences in plasma glucose or lactate levels between any treatment groups with values for all sea bass of 5.90 ± 0.43 mM and 0.45 ± 0.05 mM respectively.

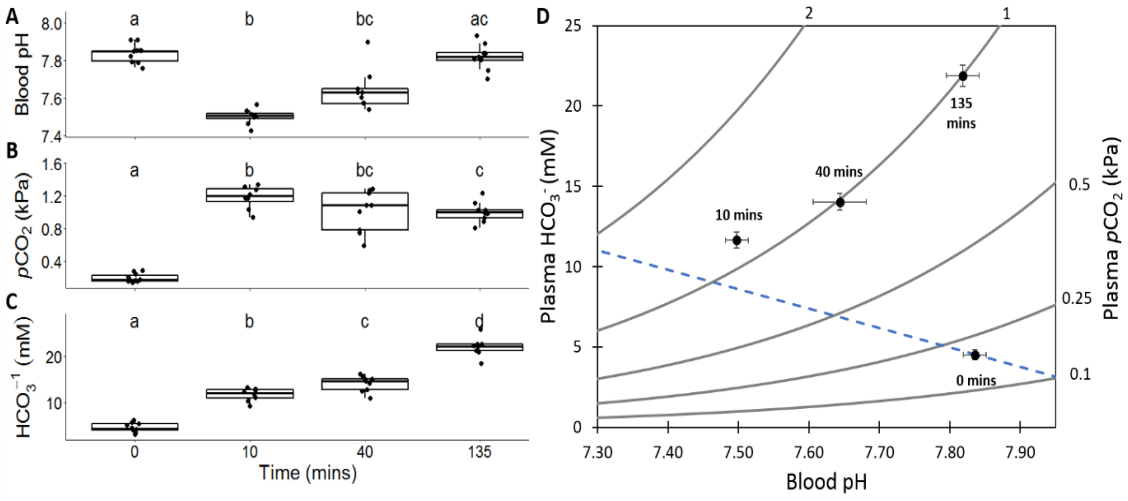

414

415 **Figure 1:** Changes in **A.** blood pH, **B.** plasma pCO_2, and **C.** plasma HCO_3^-
416 between European sea bass in control conditions (~0.05 kPa CO_2, Time = 0, n=
417 10) and after exposure to ~0.9 kPa CO_2 for ~10 minutes (n = 8), ~40 minutes (n
418 = 9), and ~135 minutes (n = 9). Significant differences between parameters at
419 each time point are indicated by different lower case letters (**A.** Dunn's test, $p <$
420 0.05; **B.** Pairwise comparison using Benjamini-Hochberg correction, $P < 0.05$ **C.**
421 Pairwise comparison of least square means, $p < 0.05$) **D.** Combined changes of
422 all three acid-base parameters are expressed as a pH/HCO_3^-/pCO_2 diagram (blue
423 dashed line indicates estimated non-bicarbonate blood buffer line based on
424 equations from Wood *et al.* (1982)) values represent mean ± s.e.m.

425 **Flux measurements**

426 Sea bass switched from slight net base excretion under control normocapnic
427 conditions to net acid excretion that was ~2.5-fold larger in magnitude during 135
428 minutes of hypercapnia (Fig. 2C, Student's t-test, $t = -2.25$, $df = 13$, $p = 0.042$).
429 This was driven by a switch from a small apparent HCO_3^- excretion to a large
430 apparent HCO_3^- uptake (Fig. 2A). There were no significant differences in T_{Amm}
431 excretion (Fig. 2B).

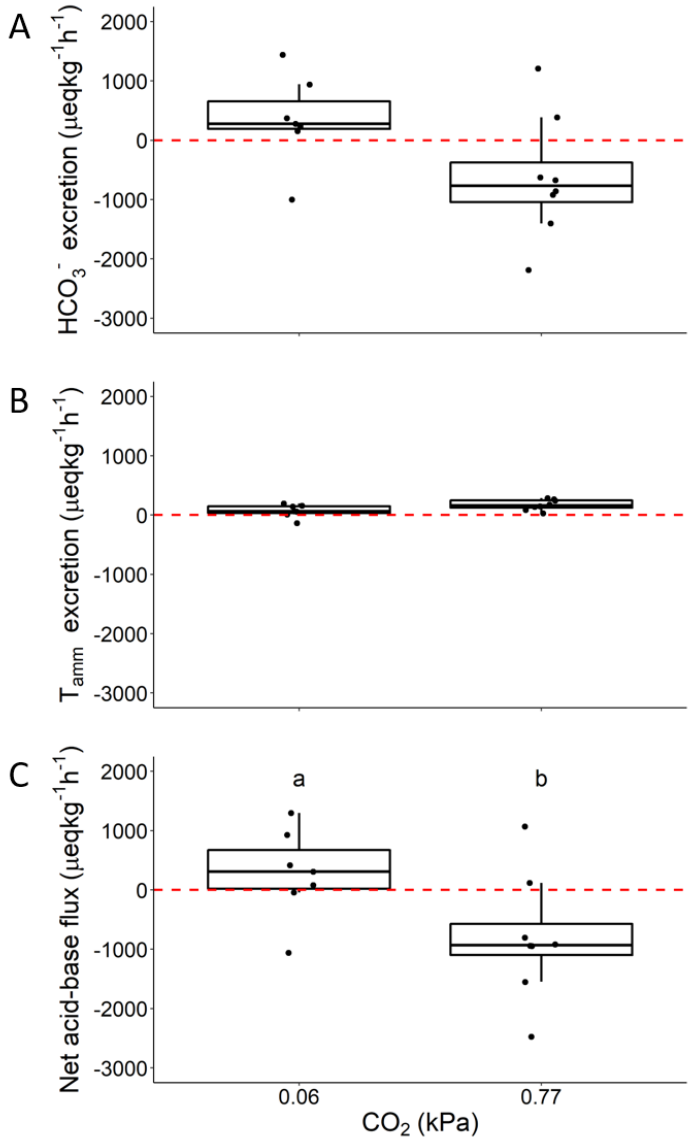

Figure 2: Changes in **A.** excretion of HCO_3^-, **B.** excretion of total ammonia (T_{amm}) and **C.** net acid-base flux between European sea bass in control conditions (n = 7, ~0.07 kPa CO_2) and after ~135 minutes exposure to hypercapnia (n = 8, ~0.84 kPa CO_2). Significant difference in parameters are indicated by different lower-case letters (Student's t-test, $p < 0.05$).

Oxygen transport capacity

The initial drop in blood pH during hypercapnia exposure was reflected in changes in erythrocyte pH_i (Fig. 3A, One-way ANOVA, $F = 12.34$, $df = 3$, $p < 0.001$) and erythrocyte $[H^+]$ (Fig. 3B, One-way ANOVA, $F = 14.64$, $df = 3$, $P < 0.001$). However, erythrocyte pH_i and $[H^+]$ returned to control levels after ~40 minutes of exposure to hypercapnia (Fig. 3A, B). As expected, the significant changes in erythrocyte pH_i and $[H^+]$ affected haemoglobin-O_2 binding affinity

leading to a ~3-fold increase in P_{50} after 10 minutes, from 1.78 kPa O_2 (± 0.30 kPa O_2) in control sea bass to 5.60 kPa O_2 (± 0.36 kPa O_2) (Kruskall-wallis test, χ^2 = 17.4, df = 3, p < 0.001). There were no changes in Hills' number across hypercapnia exposure (One-way ANOVA, F = 1.48, df = 3, p = 0.248). The rapid recovery of erythrocyte pH_i and $[H^+]$ after ~40 minutes led to P_{50} returning to pre-exposure levels (Fig. 3B).

Sea bass exposed to hypercapnia also experienced a ~25% increase in haemoglobin levels (Fig. 3D), at ~10 minutes and ~ 135 minutes compared to control sea bass (One-way ANOVA, F = 4.60, df = 3, p = 0.009). In addition, sea bass exposed to hypercapnia exhibited an ~8-10% increase in haematocrit (Fig. 3C), although this increase was marginally non-significant (One-way ANOVA, F = 2.40, df = 3, 0.086).

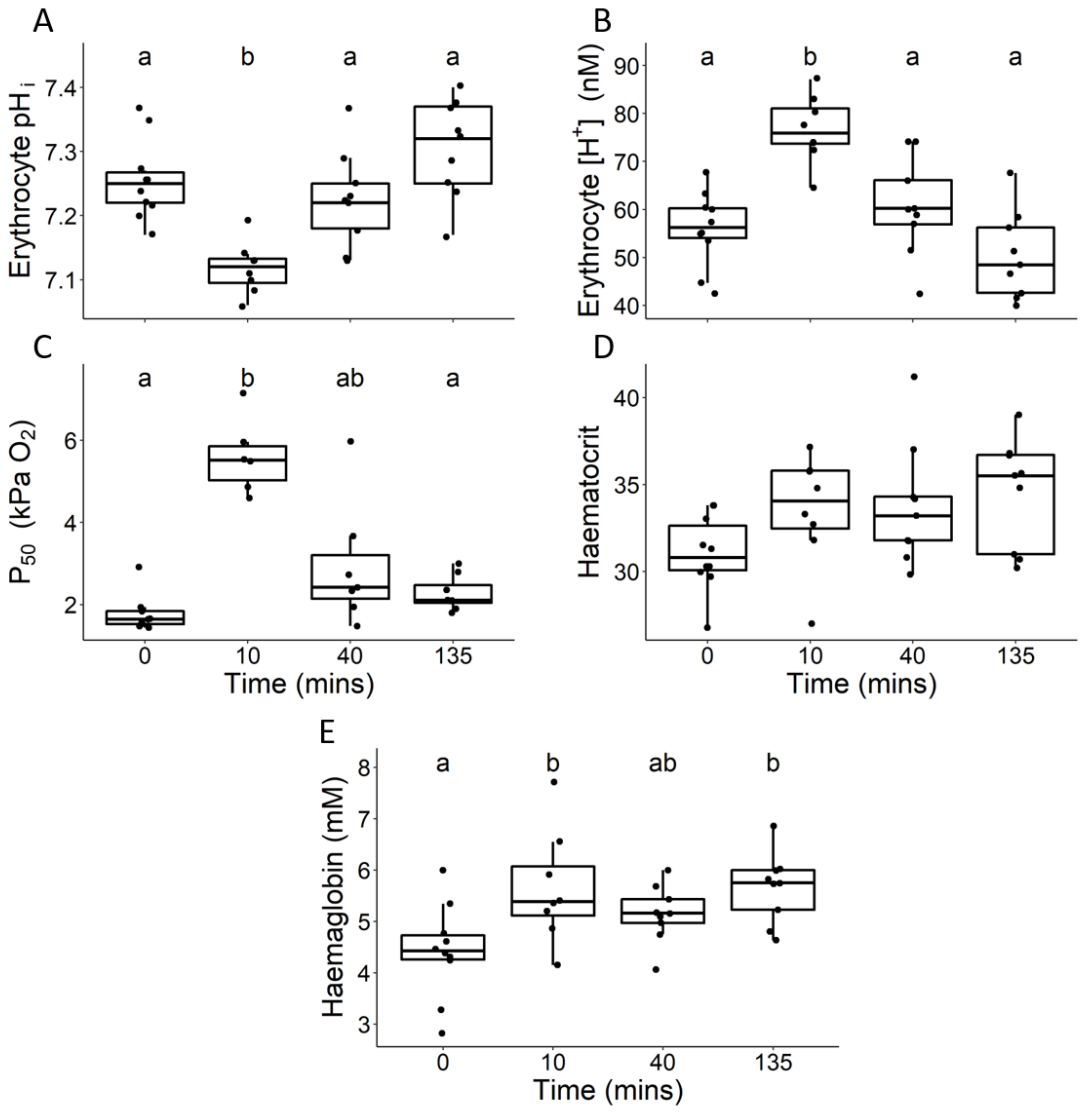

Figure 3: Changes in **A.** erythrocyte intracellular pH (erythrocyte pH_i), **B.** erythrocyte $[H^+]$, **C.** haemoglobin-O_2 binding affinity (P_{50}), **D.** haematocrit and **E.** haemoglobin level between European sea bass in control conditions (~0.05 kPa CO_2, Time = 0) and after exposure to ~0.9 kPa CO_2 for ~10 minutes, ~40 minutes, and ~135 minutes. Significant differences between parameters at each time point are indicated by different lowercase letters (**A.**, **B.**, **D.** and **E.** Pairwise comparisons of least square means, $p < 0.05$, **C.** Dunn's test, $p < 0.05$).

Response to Hypercapnia in Seawater with Low Total Alkalinity

To test the influence of environmental availability of $[HCO_3^-]$ on acid-base regulation, a group of sea bass were exposed to hypercapnia in low alkalinity seawater. These sea bass were unable to compensate for a respiratory acidosis when exposed to acute hypercapnia for ~135 minutes (Fig. 4A). Blood pH was 0.37 units (95 % CI = 0.33-0.41) lower than sea bass exposed to hypercapnia in normal alkalinity seawater for the same length of time and the same blood pH as we recorded in sea bass ~10 minutes after exposure to hypercapnia in normal seawater. Additionally, sea bass in low alkalinity seawater did not actively accumulate HCO_3^- when exposed to environmental hypercapnia for ~135 minutes (Fig. 4C). Indeed, the 11.8 mM increase in plasma $[HCO_3^-]$ (95% CI = 10.6-12.9 mM) followed the predicted non-bicarbonate buffering line (Fig. 4D).

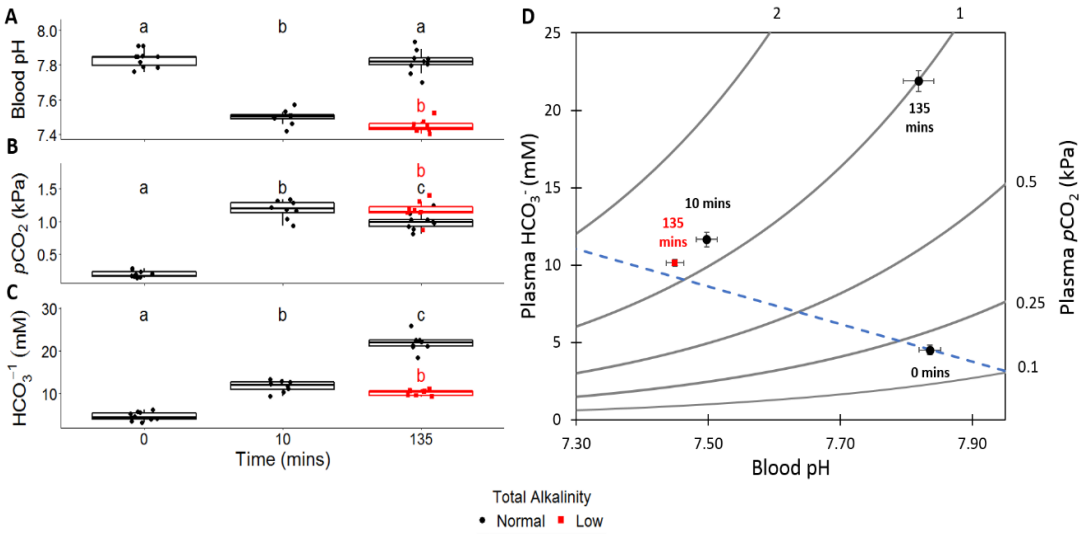

Figure 4: Comparison of **A.** blood pH, **B.** plasma pCO_2 and **C.** plasma HCO_3^- between European sea bass in control conditions (n = 10, Time = 0), exposed to hypercapnia for ~10 minutes (n = 8) in normal (~2800 µM) total alkalinity (TA) seawater, exposed to hypercapnia for ~135 minutes in normal (~2800 µM) TA

seawater (n = 9), and exposed to hypercapnia for ~135 minutes in low (~200 µM) TA seawater (n =8). Significant differences between parameters at each time point are indicated by different lower-case letters (Pairwise comparison of least squares means, $p<0.05$). For measurements taken after ~135 minutes of exposure to hypercapnia the colour indicates the TA treatment (i.e. black = normal TA, red = low TA). **D.** Combined changes of all three acid-base parameters are expressed as a pH/HCO_3^-/pCO_2 diagram (blue dashed line indicates estimated non-bicarbonate blood buffer line based on equations from Wood *et al.* (1982)) values represent mean ± s.e.m.

Plasma Ion Concentrations

Plasma [Cl^-] significantly decreased by 13.1 mM (95% CI = 10.1-16.2 mM) from 134.9 mM (± 5.1) in sea bass in normocapnia to 121.7 mM (± 1.3) in sea bass exposed to hypercapnia for ~135 minutes (Kruskall-Wallis test, $\chi^2 = 11.1$, df = 4, p = 0.025). This decrease in plasma [Cl^-] was not seen in sea bass exposed to hypercapnia in low alkalinity water (Fig. 5A). Decreases in plasma [Cl^-] showed a correlation with increasing bicarbonate (Figure 5A inset, Kendall's tau correlation, $\tau = -0.32$, p = 0.005). Plasma [Na^+] showed no significant changes over the time course of hypercapnia exposure (One-way ANOVA, F = 1.063, p = 0.391), and there were no differences in [Na^+] after ~135 minutes of exposure to hypercapnia between sea bass in normal and low TA seawater (Fig. 5B). As such, there was no correlation between plasma [Na^+] and [H^+] (Fig. 5B inset, Kendall's tau correlation, $\tau = 0.08$, p = 0.471).

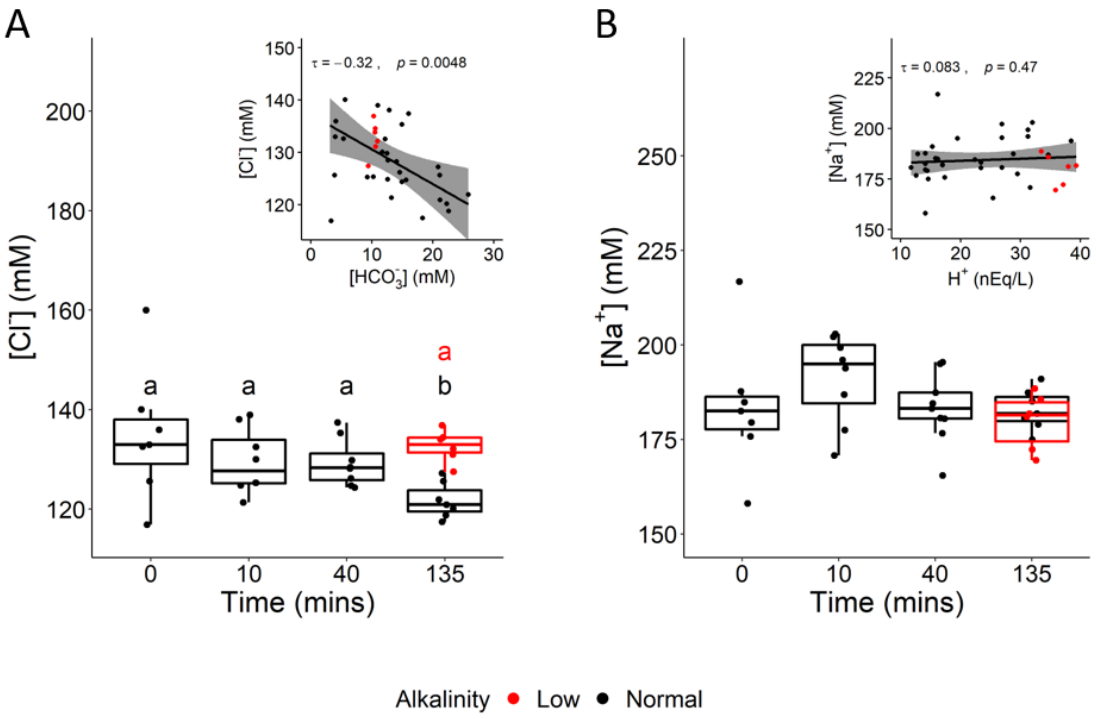

506

507 **Figure 5:** Comparison of **A.** plasma [Cl^-] and **B.** plasma [Na^+] between European
508 sea bass in control conditions (n = 7, Time = 0), exposed to hypercapnia for ~10
509 minutes (n = 8), ~40 minutes in or ~135 minutes in normal (~2800 µM) TA
510 seawater (n = 7), and exposed to hypercapnia in low (~200 µM) TA seawater (n
511 = 6). Significant differences between [Cl^-] at each time point are indicate by
512 different lower-case letters (Pairwise comparison of least squares means,
513 $p<0.05$). Insets show correlation between **A.** plasma [Cl^-] and [HCO_3^-]. **B.** plasma
514 [Na^+] and [H^+]. T and p value shown represent results of Kendall's tau correlation.
515 Shaded area represents 95% CI of linear regression between measures. For
516 insets and measurements taken after ~135 minutes of exposure to hypercapnia
517 the colour indicates the TA treatment (i.e. black = normal TA, red = low TA).

518 **NKA and NHE3 Protein Abundance**

519 Exposure to hypercapnia did not induce significant changes in the abundance
520 of NKA or NHE3 in crude homogenates (indicative of total protein abundance) or
521 the abundance of NKA and NHE3 in membrane-enriched fractions (indicative of
522 protein that was present in the apical or basolateral plasma membranes) (One-
523 tailed t-test, $P > 0.05$; Fig. 6).

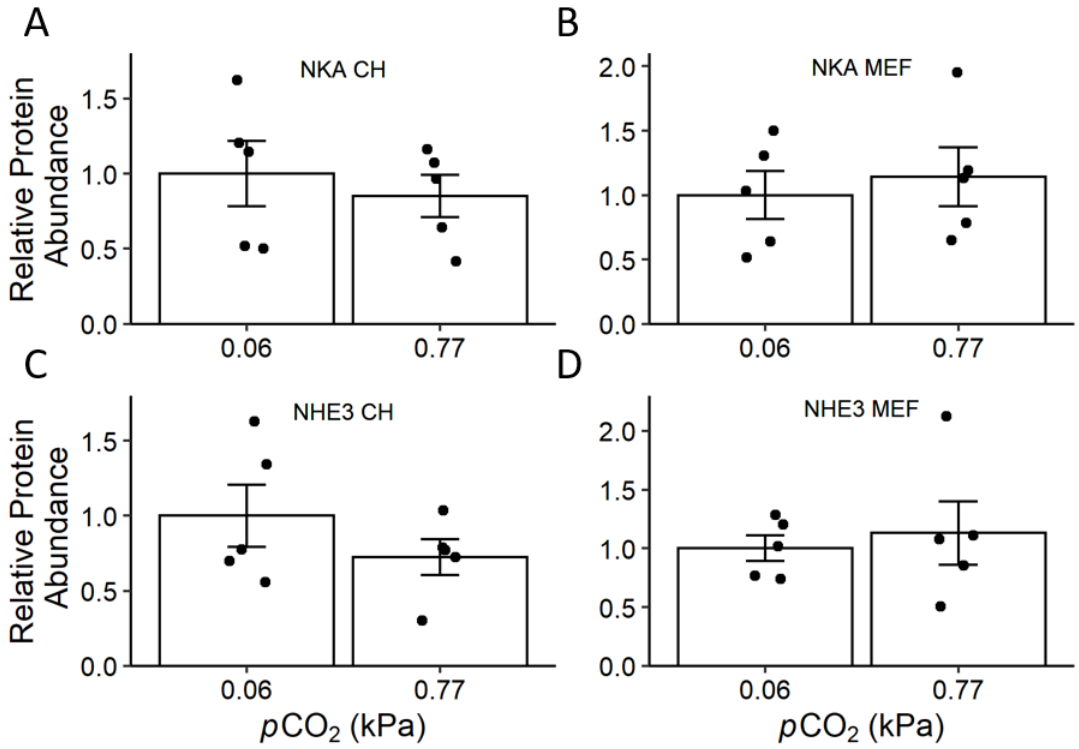

Figure 6: Comparison of gill **A.** Na^+/K^+-ATPase (NKA) in crude homogenates (CH), **B.** NKA in the membrane-enriched fraction (MEF) as well as **C.** Na^+/H^+ Exchanger 3 (NHE3) CH, and **D.** NHE3 MEF abundance between European sea bass exposed to control conditions (~0.06 kPa CO_2) and to hypercapnia (~0.77 kPa CO_2) for ~135 minutes (n = 5 per treatment, 1-tailed t-test). Bars show mean ± s.e.m., points show raw data; there were no significant differences between any measurements (1-tailed t-tests, $p > 0.05$).

Ionocyte Intracellular Localisation and Apical Surface Area

NKA-rich ionocytes were primarily localised on the gill filament trailing edges and the basal portion of the gill lamellae (Fig. S1), all NKA-rich ionocytes also expressed NHE3 in their apical region (Fig. 7A). Despite analysis using high magnification imaging, optical sectioning, and XZ- and YZ-plane visualization, we found no evidence of NHE3 intracellular localisation (Figure 7B, B', C, C'). The ionocyte's apical surface area (based on the NHE3 signal) significantly increased, almost doubling from 3.38 ± 0.41 to 6.45 ± 0.64 μm^2, after exposure to ~135 min of hypercapnia (one-tailed t-test, $t = 4.048$, $df = 6.828$, $p = 0.003$; Fig. 7D).

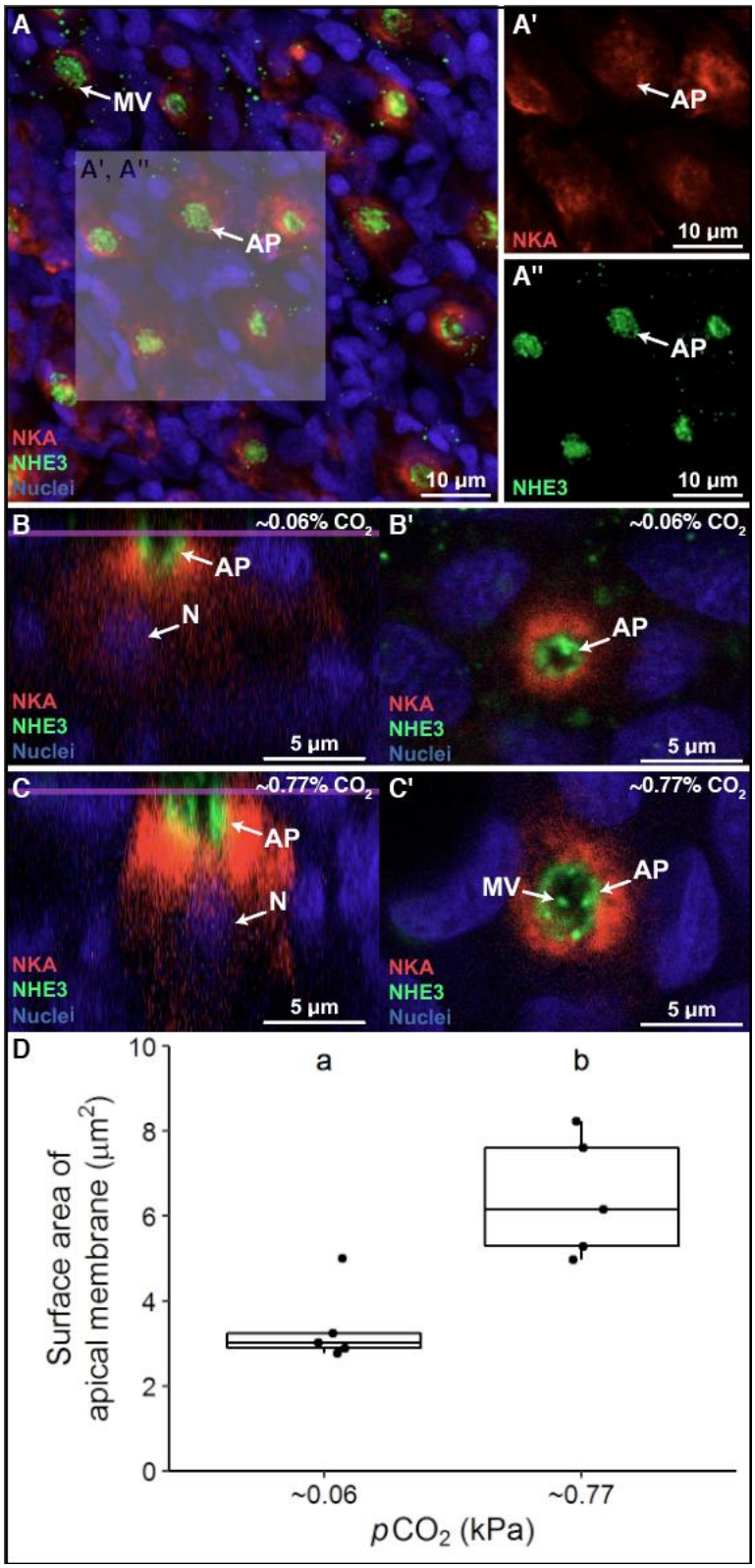

Figure 7: **A.** The European sea bass' gill ionocytes express abundant **A'.** basolateral Na^+/K^+-ATPase (NKA, red) and **A''.** apical Na^+/H^+ Exchanger 3 (NHE3, green). Comparison of gill ionocytes between European sea bass exposed to **B, B'.** control conditions (~0.06 kPa CO_2) and **C, C'.** to ~0.77 kPa CO_2

for ~135 minutes revealed no changes in intracellular localisation, but determined **D.** hypercapnia-exposed sea bass had significantly wider apical surface area (n = 5 per treatment, 1-tailed t-test, p = 0.003). The purple line in **B** and **C** denotes the slice at which **B'** and **C'** were imaged. Nuclei (blue) are stained with DAPI.

Discussion

Our results indicate that European sea bass are able to rapidly compensate for hypercapnia-induced blood acidosis when the environmental CO_2 is at the extreme high end of the spectrum encountered in their natural habitat. Complete restoration of blood pH after exposure to ~1 kPa CO_2 was achieved within ~2 hours via a switch from net base excretion to net acid excretion and a subsequent accumulation of HCO_3^- in plasma. In addition, erythrocyte pH_i and Hb-O_2 affinity were restored to pre-exposure levels after just ~40 min, and there was a 20% increase in the blood haemoglobin concentration together with a trend for ~10% haematocrit increase. These results suggest an adrenergic response that stimulates a β-NHEs in the erythrocytes (Nikinmaa, 2012), and contracts the spleen resulting in the release of erythrocytes into the circulation (Crocker and Cech, 1997; Lee et al., 2003; Perry and Kinkead, 1989; Vermette and Perry, 1988). The end result is a boost in blood O_2 transport capacity that counteracts the reduced Hb-O_2 affinity induced by the initial hypercapnia-induced acidosis.

Regulation of respiratory acidosis by sea bass exposed to hypercapnia in normal alkalinity sea water (TA ~2,800 µM) resulted in an elevation of plasma $[HCO_3^-]$ by ~18 mM, which was correlated with a decrease in plasma $[Cl^-]$ of ~13 mM. In comparison, while we saw a slight rise in plasma $[Na^+]$ on initial exposure to hypercapnia, this was transient, and there was no overall correlation between plasma $[Na^+]$ and $[H^+]$ during the whole 135 minute experiment. However, a lack of increase in plasma $[Na^+]$ during acid-base regulation does not preclude increased Na^+ uptake (to facilitate H_+ excretion) during acid-base regulation. Instead, a lack of increased plasma $[Na^+]$ may simply reflect upregulation of the hypo-ionoregulatory mechanism for NaCl excretion in marine teleosts (Liu et al., 2016), which would presumably occur to compensate for enhanced uptake of Na^+ to facilitate H^+ excretion by NHE. This would also help explain the observed reduction in plasma $[Cl^-]$ in fish exposed to hypercapnia.

In comparison, sea bass exposed to hypercapnia in low alkalinity sea water (TA ~200 µM) showed no ability to accumulate HCO_3^-, to compensate for respiratory acidosis, and did not experience a decrease in plasma [Cl^-]. At face value, these results may support potential direct uptake of HCO_3^- from seawater in exchange for blood Cl^- through HCO_3^-/Cl^- exchange across the gills (Esbaugh et al., 2012; Perry and Gilmour, 2006; Tovey and Brauner, 2018). However, the thermodynamics of this proposed mechanism are not clear, as [Cl^-] is much higher in seawater than in internal fluids of fish, and the opposite is true for [HCO_3^-]. This implies that both counterions would have to be transported against their concentration gradients, and furthemore, these gradients would become increasingly unfavourable as blood acidosis is compensated. Importantly, our hypercapnic low alkalinity seawater had a pH of ~5.7, which was ~1.2 pH units lower than hypercapnic normal alkalinity seawater (a 15-fold increase in [H^+]). Based on nominal values of [Na^+] and [H^+] inside fish gill ionocytes and calculations in Parks *et al.* (2008), the low alkalinity seawater would not sustain H^+ excretion via NHEs (Table S5). Interestingly, as Na^+ excretion is coupled to Cl^- excretion (via pathways independent of NHE), inactivation of NHE would also explain the lack of increase of plasma [Cl^-] in low alkalinity sea water. Overall, this evidence supports enhanced NHE mediated H^+ excretion (resulting in retention of metabolically produced HCO_3^- in the blood), rather than direct HCO_3^- uptake from sea water, as the primary mechanism underlying regulation of respiratory acidosis in sea bass.

To investigate the mechanisms used by sea bass to enhance acid-excretion, we examined whether changes in gill NKA and NHE3 occur after acute (~135 minute) exposure to hypercapnia. Gill NKA and NHE3 protein abundance did not change, ruling out increased protein synthesis as the mechanism responsible for the observed upregulation in acid-excretion; this is not surprising considering the short timeframe of our experiments. We also examined the potential translocation of pre-existing NKA and NHE3 to the ionocyte basolateral and apical membranes, respectively. Such mechanisms upregulate acid-base regulatory ion transport in elasmobranchs (Roa et al., 2014; Tresguerres et al., 2005; Tresguerres et al., 2006; Tresguerres et al., 2007b) and hagfish (Parks et al., 2007; Tresguerres et al., 2007a); however, NKA and NHE3 protein abundance in the gill membrane fraction of European sea bass gills was also unchanged, ruling out NKA and NHE3 translocation in our experiments. Finally, we hypothesized that sea bass

could have remodelled the apical membrane of ionocytes to increase the sites for H^+ excretion in contact with seawater. Indeed, this was the case as the surface area of the NHE3-abundant apical membrane of NKA-rich ionocytes roughly doubled in response to hypercapnia.

Previous studies on freshwater fishes have also documented morphological adjustments in gill ionocytes upon comparable hypercapnic exposures. However, the responses were the opposite to our study, as those freshwater fishes experienced a significant reduction in ionocyte apical surface area (Baker et al., 2009a; Goss et al., 1992b; Leino and McCormick, 1984). In some cases, the apical membrane retracted into a more pronounced apical pit (Goss et al., 1992a; Goss et al., 1994), which was suggested to create a microenvironment with higher [Na^+] compared to the bulk freshwater and facilitate Na^+/H^+ exchange (Kumai and Perry, 2012). However, exposure to more pronounced hypercapnia (8 kPa CO_2 over four days) induced an increase in gill ionocyte apical surface area in freshwater catfish (*Ictalurus punctatus*) (Cameron and Iwama, 1987). This response was similar to the seabass in our study; however, the longer time frame likely allowed for additional responses that were not investigated, such as increased synthesis of ion-transporting proteins or a change in the H^+ excreting mechanism. In any case, the ability of seabass to rapidly compensate a blood respiratory acidosis by increasing gill ionocyte apical surface area is in large part possible due to the overabundance of Na^+ in sea water, which establishes favourable conditions for NHE-mediated H^+ excretion.

Freshwater species typically take from 24 h to > 72 h to regulate blood pH after exposure to 1 kPa CO_2 (Baker et al., 2009a; Claiborne and Heisler, 1984; Claiborne and Heisler, 1986; Damsgaard et al., 2015; Larsen and Jensen, 1997; Perry, 1982; Perry et al., 1981; Smatresk and Cameron, 1982). While it is generally believed that marine teleosts can regulate their blood acid-base status at a faster rate than freshwater species (Brauner et al., 2019), relatively little research has been conducted to characterise the speed of acid-base regulation in marine fish. A bibliography search revealed four previous studies on five marine teleost species that characterized the time course of the acid-base regulatory response after exposure to 1 kPa CO_2 (Fig. 8). Of these species, only the Japanese amberjack (*Seriola quinqueradiata*) was able to restore blood pH_e

faster than sea bass (~60 min vs ~135 min; Fig. 8B). The remaining four species regulated blood pH_e between 3 and 24 h post CO_2 exposure (Figure 8C, D, E, F).

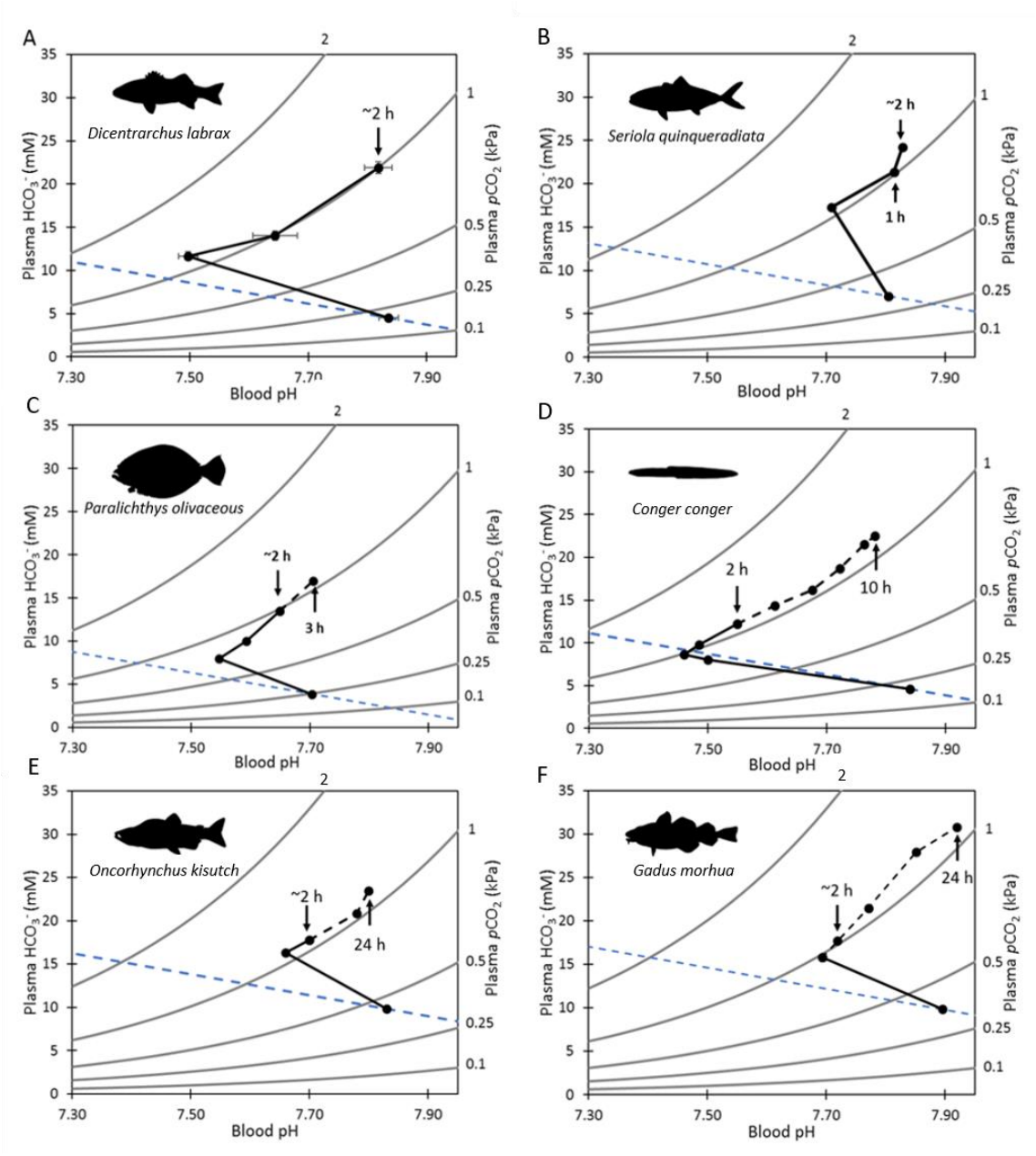

Figure 8: Blood pH/HCO_3^-/pCO_2 plots for **A.** European sea bass, *Dicentrarchus labrax* (Present study), **B.** Japanese amberjack, *Seriola quinqeradiata* (Hayashi *et al.*, 2004, re-plotted raw data provided by pers. comm. with Dr Atsushi Ishimatsu, Can Tho University), **C.** Japanese flounder, *Paralichthys olivaceus* (Hayashi et al., 2004), **D.** conger eel, *Conger conger* (Toews et al., 1983), **E.** coho salmon, *Oncorhynchus kisutch* (Perry, 1982), and **F.** Atlantic cod, *Gadus morhua* (Larsen et al., 1997). The corresponding blood pH and HCO_3^- of each species at a time ~2 h after 1 kPa CO_2 exposure is indicated to allow direct comparisons with European sea bass. Times below the relevant

point indicate when blood pH was not statistically different from pre-exposure levels for each species. The time course of the acid-base response after 2 h is indicated by a dashed black line. The dashed blue line is an approximated non-HCO_3^- buffer line based on the mean haematocrit of sea bass from the present study and calculated using the equation for rainbow trout from Wood *et al.* (1982).

The robust ability of sea bass to rapidly acid-base regulate in response hypercapnia likely plays a significant role in their natural environment. Specifically, sea bass feed in shallow coastal estuaries and salt marsh habitats during the summer (Doyle et al., 2017), and these habitats typically experience large fluctuations in CO_2 levels over short time periods (Hofmann et al., 2011; Melzner et al., 2013; Wallace et al., 2014). For example, equivalent salt marshes on the US coast regularly experience CO_2 fluctuations of ~0.4 kPa across tide cycles during the summer (Baumann et al., 2015). The fast acid-base regulatory response observed in our study indicates that sea bass would be able to rapidly correct the respiratory blood acidosis caused by this level of CO_2 variation in <1 hour. Critically, regulation of erythrocyte pH_i by sea bass was the fastest recorded in any fish species. By rapidly restoring erythrocyte pH_i O_2 transport capacity is maintained, which is crucial for active predatory teleosts. However, environmental CO_2 variation cannot be the sole driver for enhanced acid-base regulatory capacities in all species. For example, Japanese amberjack show a similarly fast blood acid-base regulatory response (Hayashi et al., 2004) but primarily inhabit pelagic, offshore ecosystems in which large variation in environmental CO_2 may be less likely to occur. An alternative may be that active, predatory species have developed higher capacities for acid-base regulation to deal with large metabolic acidosis (as a result of anaerobic respiration used during intense exercise involved in prey capture). Understanding the mechanisms that determine species-specific differences in acid-base regulatory capacity will help understand differential impacts of acute exposure to elevated CO_2, both by itself and in combination with other stressors such as hypoxia. For example, we have recently reported that sea bass showed enhanced hypoxia tolerance when exposed to progressive and environmentally relevant hypercapnia and hypoxia over a 6 hour period (Montgomery et al., 2019). In contrast, European plaice (*Pleuronectes platessa*) and European flounder (*Platichthys flesus*) exposed to the same conditions showed reduced hypoxia tolerance (P_{crit}), which was associated with reduced Hb-O_2 affinity and O_2 uptake

resulting from an uncompensated respiratory acidosis (Rogers, 2015; Montgomery *et al.* unpublished observations). Thus, species with more robust acid-base regulatory mechanisms seem more resilient to interactive effects between hypercapnia and hypoxia.

Conclusion

Overall, our study highlights the capacity of European sea bass to rapidly (2 hours) regulate blood and erythrocyte acid-base status and O_2 transport capacity upon exposure to a pronounced and sudden increase in environmental CO_2 levels. Sea bass' ability to rapidly upregulate H^+ excretion appears to be mediated via the increased exposure of NHE3-containing apical surface area of gill ionocytes, rather than changes in NHE3 or NKA protein abundance or localisation. Additionally, sea bass erythrocyte pH_i is regulated even more rapidly than blood pH (40 minutes), which enables them to quickly restore the affinity of haemoglobin for O_2, and therefore blood O_2 transport capacity during exposure to elevated CO_2. In conjunction, these acid-base regulatory responses will minimise the impact of pronounced and rapidly fluctuating CO_2 in their natural environments, and so may prevent disruption of energetically costly activities such as foraging or digestion, and may make sea bass more resilient to impacts of hypoxia and additional stressors during acute periods of hypercapnia. This is an avenue where we believe further research effort is necessary.

Conflict of Interest: The authors declare no conflicts of interest.

Author contributions: D.W.M. designed the experiment, performed all data collection and analysis other than for gill samples, and wrote the manuscript. W.D., J.F., and A.B assisted with data collection, data analysis and editing of the manuscript. R.W.W. supervised the study and assisted with designing the experiments, data collection and analysis, and writing of the manuscript. S.D.S., G.H.E., and S.N.R.B. assisted with data analysis and editing of the manuscript. G.T.K. conducted all data analysis of gill samples and assisted with writing the manuscript. M.T. assisted with data analysis and writing of the manuscript.

Acknowledgements: This work was supported by a NERC GW4+ Doctoral Training Partnership studentship from the Natural Environment Research Council [NE/L002434/1] with additional funding from CASE partner, The Centre for Environment, Fisheries and Aquaculture Science (Cefas) to D.W.M., and from

the Biotechnology and Biological Sciences Research Council (BB/D005108/1 and BB/J00913X/1) and NERC (NE/H017402/1) to R.W.W. G.T.K. was funded by the National Science Foundation (NSF) Postdoctoral Fellowship Program (#1907334). M.T. received funding from NSF IOS #1754994. We thank Dr Junya Hiroi for providing the NHE3 antibodies, and Dr Andrew Esbaugh and Dr Till Harter for discussions related to data interpretation. We would similarly like to thank the aquarium staff, particularly Dr Gregory Paul, Paul Tyson, Rebecca Turner, Alex Bell, and Richard Silcox, of the Aquatic Resource Centre at the University of Exeter for assistance with fish husbandry and maintenance of aquarium facilities.

Data availability: Data will be deposited on the University of Exeter's Open Research Exeter (ORE) depository and a URL to the dataset provided prior to article acceptance or upon request by reviewers.

References

Baker, D. W., Matey, V., Huynh, K. T., Wilson, J. M., Morgan, J. D. and Brauner, C. J. (2009a). Complete intracellular pH protection during extracellular pH depression is associated with hypercarbia tolerance in white sturgeon, Acipenser transmontanus. *Am. J. Physiol. Integr. Comp. Physiol.* **296**, R1868–R1880.

Baker, D. W., May, C. and Brauner, C. J. (2009b). A validation of intracellular pH measurements in fish exposed to hypercarbia: the effect of duration of tissue storage and efficacy of the metabolic inhibitor tissue homogenate method. *J. Fish Biol.* **75**, 268–275.

Baumann, H., Wallace, R. B., Tagliaferri, T. and Gobler, C. J. (2015). Large Natural pH, CO2 and O2 Fluctuations in a Temperate Tidal Salt Marsh on Diel, Seasonal, and Interannual Time Scales. *Estuaries and Coasts* **38**, 220–231.

Blondeau-Bidet, E., Hiroi, J. and Lorin-Nebel, C. (2019). Ion uptake pathways in European sea bass Dicentrarchus labrax. *Gene* **692**, 126–137.

Borges, A. V, Schiettecatte, L.-S., Abril, G., Delille, B. and Gazeau, F. (2006). Carbon dioxide in European coastal waters. *Estuar. Coast. Shelf Sci.* **70**, 375–387.

Boutilier, R. G., Heming, T. A. and Iwama, G. K. (1984). Appendix: Physicochemical Parameters for use in Fish Respiratory Physiology**The authors were supported by N.S.E.R.C. (Canada). In *Fish Physiology* (ed. Hoar, W. S.) and Randall, D. J.), pp. 403–430. Academic Press.

Boutilier, R. G., Iwama, G. K., Heming, T. A. and Randall, D. J. (1985). The apparent pK of carbonic acid in rainbow trout blood plasma between 5 and 15°C. *Respir. Physiol.* **61**, 237–254.

Brauner, C. J. and Baker, D. W. (2009). Patterns of Acid–Base Regulation During Exposure to Hypercarbia in Fishes BT - Cardio-Respiratory Control in Vertebrates: Comparative and Evolutionary Aspects. In (ed. Glass, M. L.) and Wood, S. C.), pp. 43–63. Berlin, Heidelberg: Springer Berlin Heidelberg.

Brauner, C. J., Shartau, R. B., Damsgaard, C., Esbaugh, A. J., Wilson, R. W. and Grosell, M. (2019). 3 - Acid-base physiology and CO_2 homeostasis: Regulation and compensation in response to elevated environmental CO_2. In *Carbon Dioxide* (ed. Grosell, M.), Munday, P. L.), Farrell, A. P.), and Brauner, C. J. B. T.-F. P.), pp. 69–132. Academic Press.

Cai, W.-J., Hu, X., Huang, W.-J., Murrell, M. C., Lehrter, J. C., Lohrenz, S. E., Chou, W.-C., Zhai, W., Hollibaugh, J. T., Wang, Y., et al. (2011). Acidification of subsurface coastal waters enhanced by eutrophication. *Nat. Geosci* **4**, 766–770.

Cameron, J. N. and Iwama, G. K. (1987). Compensation of Progressive Hypercapnia in Channel Catfish and Blue Crabs. *J. Exp. Biol.* **133**, 183 LP – 197.

Claiborne, J. B. and Heisler, N. (1984). Acid-Base Regulation and Ion Transfers in the Carp (*Cyprinus Carpio*) During and After Exposure to Environmental Hypercapnia. *J. Exp. Biol.* **108**, 25 LP – 43.

Claiborne, J. B. and Heisler, N. (1986). Acid-base regulation and ion transfers in the carp (*Cyprinus carpio*): pH compensation during graded long- and short-term environmental hypercapnia, and the effect of bicarbonate infusion. *J. Exp. Biol.* **126**, 41 LP – 61.

Claiborne, J. B., Edwards, S. L. and Morrison-Shetlar, A. I. (2002). Acid–base regulation in fishes: cellular and molecular mechanisms. *J. Exp. Zool.* **293**, 302–319.

Cooper, C. A., Whittamore, J. M. and Wilson, R. W. (2010). Ca2+-driven intestinal HCO3− secretion and CaCO3 precipitation in the European flounder in vivo: influences on acid-base regulation and blood gas transport. *Am. J. Physiol. Integr. Comp. Physiol.* **298**, R870–R876.

Cossins, A. R. and Richardson, P. A. (1985). Adrenalin-Induced Na+/H+ Exchange in' Trout Erythrocytes and its Effects Upon Oxygen-Carrying Capacity. *J. Exp. Biol.* **118**, 229 LP – 246.

Crocker, C. E. and Cech, J. J. (1997). Effects of environmental hypoxia on oxygen consumption rate and swimming activity in juvenile white sturgeon, *Acipenser transmontanus*, in relation to temperature and life intervals. *Environ. Biol. Fishes* **50**, 383–389.

Crocker, C. E. and Cech Jr, J. J. (1998). Effects of hypercapnia on blood-gas and acid-base status in the white sturgeon, Acipenser transmontanus. *J. Comp. Physiol. B* **168**, 50–60.

Damsgaard, C., Gam, L. T. H., Tuong, D. D., Thinh, P. V., Huong Thanh, D. T., Wang, T. and Bayley, M. (2015). High capacity for extracellular acid–base regulation in the air-breathing fish *Pangasianodon hypophthalmus*. *J. Exp. Biol.* **218**, 1290 LP – 1294.

Dickson, A. G. and Millero, F. J. (1987). A comparison of the equilibrium constants for the dissociation of carbonic acid in seawater media. *Deep Sea Res. Part A. Oceanogr. Res. Pap.* **34**, 1733–1743.

Dickson, A. G., Sabine, C. L. and Christian, J. R. (2007). *Guide to best practices for ocean CO2 measurements.* North Pacific Marine Science Organization.

Doney, S. C., Fabry, V. J., Feely, R. A. and Kleypas, J. A. (2009). Ocean Acidification: The Other CO_2 Problem. *Ann. Rev. Mar. Sci.* **1**, 169–192.

Doyle, T. K., Haberlin, D., Clohessy, J., Bennison, A. and Jessopp, M. (2017). Localised residency and inter-annual fidelity to coastal foraging areas may place sea bass at risk to local depletion. *Sci. Rep.* **7**, 45841.

Eddy, F. B., Lomholt, J. P., Weber, R. E. and Johansen, K. (1977). Blood respiratory properties of rainbow trout (Salmo gairdneri) kept in water of high CO2 tension. *J. Exp. Biol.* **67**, 37 LP – 47.

Esbaugh, A. J. (2017). Physiological implications of ocean acidification for marine fish: emerging patterns and new insights. *J. Comp. Physiol. B* 1–13.

Esbaugh, A. J., Heuer, R. and Grosell, M. (2012). Impacts of ocean acidification on respiratory gas exchange and acid-base balance in a marine teleost, Opsanus beta. *J. Comp. Physiol. B.* **182**, 921–934.

Evans, D. H., Piermarini, P. M. and Choe, K. P. (2005). The Multifunctional Fish Gill: Dominant Site of Gas Exchange, Osmoregulation, Acid-Base Regulation, and Excretion of Nitrogenous Waste. *Physiol. Rev.* **85**, 97–177.

Goss, G. G., Laurent, P. and Perry, S. F. (1992a). Evidence for a morphological component in acid-base regulation during environmental hypercapnia in the brown bullhead (Ictalurus nebulosus). *Cell Tissue Res.* **268**, 539–552.

Goss, G. G., Perry, S. F., Wood, C. M. and Laurent, P. (1992b). Mechanisms of ion and acid-base regulation at the gills of freshwater fish. *J. Exp. Zool.* **263**, 143–159.

Goss, G. G., Laurent, P. and Perry, S. F. (1994). Gill morphology during hypercapnia in brown bullhead (Ictalurus nebulosus): role of chloride cells and pavement cells in acid-base regulation. *J. Fish Biol.* **45**, 705–718.

Hayashi, M., Kita, J. and Ishimatsu, A. (2004). Acid-base responses to lethal aquatic hypercapnia in three marine fishes. *Mar. Biol.* **144**, 153–160.

Hofmann, G. E., Smith, J. E., Johnson, K. S., Send, U., Levin, L. A., Micheli, F., Paytan, A., Price, N. N., Peterson, B. and Takeshita, Y. (2011). High-frequency dynamics of ocean pH: a multi-ecosystem comparison. *PLoS One* **6**,.

Kumai, Y. and Perry, S. F. (2012). Mechanisms and regulation of Na+ uptake by freshwater fish. *Respir. Physiol. Neurobiol.* **184**, 249–256.

Kwan, G. T., Wexler, J. B., Wegner, N. C. and Tresguerres, M. (2019). Ontogenetic changes in cutaneous and branchial ionocytes and morphology in yellowfin tuna (Thunnus albacares) larvae. *J. Comp. Physiol. B* **189**, 81–95.

Kwan, G. T., Smith, T. R. and Tresguerres, M. (2020). Immunological characterization of two types of ionocytes in the inner ear epithelium of Pacific Chub Mackerel (Scomber japonicus). *J. Comp. Physiol. B* **190**, 419–431.

Larsen, B. K. and Jensen, F. B. (1997). Influence of ionic composition on acid-base regulation in rainbow trout (Oncorhynchus mykiss) exposed to environmental hypercapnia. *Fish Physiol. Biochem.* **16**, 157–170.

Larsen, B. K., Pörtner, H. O. and Jensen, F. B. (1997). Extra- and intracellular acid-base balance and ionic regulation in cod (Gadus morhua) during combined and isolated exposures to hypercapnia and copper. *Mar. Biol.* **128**, 337–346.

Lebovitz, R. M., Takeyasu, K. and Fambrough, D. M. (1989). Molecular characterization and expression of the (Na+ + K+)-ATPase alpha-subunit in Drosophila melanogaster. *EMBO J.* **8**, 193–202.

Lee, K.-S., Kita, J. and Ishimatsu, A. (2003). Effects of Lethal Levels of Environmental Hypercapnia on Cardiovascular and Blood-Gas Status in Yellowtail, *Seriola quinqueradiata*. *Zoolog. Sci.* **20**, 417–422.

Leino, R. L. and McCormick, J. H. (1984). Morphological and morphometrical changes in chloride cells of the gills of Pimephales promelas after chronic exposure to acid water. *Cell Tissue Res.* **236**, 121–128.

Lenth, R. (2020). emmeans: Estimated Marginal Means, aka Least-Squares Means.

Lewis, C., Clemow, K. and Holt, W. V (2013). Metal contamination increases the sensitivity of larvae but not gametes to ocean acidification in the polychaete Pomatoceros lamarckii (Quatrefages). *Mar. Biol.* **160**, 2089–2101.

Liu, S.-T., Horng, J.-L., Chen, P.-Y., Hwang, P.-P. and Lin, L.-Y. (2016). Salt secretion is linked to acid-base regulation of ionocytes in seawater-acclimated medaka: new insights into the salt-secreting mechanism. *Sci. Rep.* **6**, 31433.

McDonald, D. G. and Wood, C. M. (1981). Branchial and Renal Acid and Ion Fluxes in the Rainbow Trout, Salmo Gairdneri, at Low Environmental pH. *J. Exp. Biol.* **93**, 101 LP – 118.

Melzner, F., Thomsen, J., Koeve, W., Oschlies, A., Gutowska, M. A., Bange, H. W., Hansen, H. P. and Körtzinger, A. (2013). Future ocean acidification will be amplified by hypoxia in coastal habitats. *Mar. Biol.* **160**, 1875–1888.

Middlemiss, K. L., Urbina, M. A. and Wilson, R. W. (2016). Effects of seawater alkalinity on calcium and acid–base regulation in juvenile European lobster (Homarus gammarus) during a moult cycle. *Comp. Biochem. Physiol. Part A Mol. Integr. Physiol.* **193**, 22–28.

Montgomery, D. W., Simpson, S. D., Engelhard, G. H., Birchenough, S. N. R. and Wilson, R. W. (2019). Rising CO_2 enhances hypoxia tolerance in a marine fish. *Sci. Rep.* **9**, 15152.

Motulsky, H. J. and Brown, R. E. (2006). Detecting outliers when fitting data

with nonlinear regression – a new method based on robust nonlinear regression and the false discovery rate. *BMC Bioinformatics* **7**, 123.

Nadler, L. E., Bengston, E., Eliason, E. J., Hassibi, C., Helland-Riise, S. H., Johansen, I. B., Kwan, G. T., Tresguerres, M., Turner, A. V, Weinersmith, K. L., et al. (2021). A brain-infecting parasite impacts host metabolism both during exposure and after infection is established. *Funct. Ecol.* **35**, 105–116.

Nikinmaa, M. (2012). *Vertebrate red blood cells: adaptations of function to respiratory requirements*. Springer Science & Business Media.

Nikinmaa, M. and Tufts, B. L. (1989). Regulation of acid and ion transfer across the membrane of nucleated erythrocytes. *Can. J. Zool.* **67**, 3039–3045.

Oellermann, M., Pörtner, H. O. and Mark, F. C. (2014). Simultaneous high-resolution pH and spectrophotometric recordings of oxygen binding in blood microvolumes. *J. Exp. Biol.* **217**, 1430 LP – 1436.

Ogle, D. H., Wheeler, P. and Dinno, A. (2020). FSA: Fisheries Stock Analysis.

Pan, T.-C. F., Applebaum, S. L. and Manahan, D. T. (2015). Experimental ocean acidification alters the allocation of metabolic energy. *Proc. Natl. Acad. Sci.* **112**, 4696 LP – 4701.

Parks, S. K., Tresguerres, M. and Goss, G. G. (2007). Blood and gill responses to HCl infusions in the Pacific hagfish (Eptatretus stoutii). *Can. J. Zool.* **85**, 855–862.

Parks, S. K., Tresguerres, M. and Goss, G. G. (2008). Theoretical considerations underlying Na+ uptake mechanisms in freshwater fishes. *Comp. Biochem. Physiol. Part C Toxicol. Pharmacol.* **148**, 411–418.

Perry, S. F. (1982). The regulation of hypercapnic acidosis in two Salmonids, the freshwater trout (Salmo gairdneri) and the seawater salmon (Onchorynchus kisutch). *Mar. Behav. Physiol.* **9**, 73–79.

Perry, S. F. and Gilmour, K. M. (2006). Acid–base balance and CO2 excretion in fish: Unanswered questions and emerging models. *Respir. Physiol. Neurobiol.* **154**, 199–215.

Perry, S. F. and Kinkead, R. (1989). The role of catecholamines in regulating arterial oxygen content during acute hypercapnic acidosis in rainbow trout (Salmo gairdneri). *Respir. Physiol.* **77**, 365–377.

Perry, S. F. and McKendry, J. E. (2001). The relative roles of external and internal CO₂ versus H⁺ in eliciting the cardiorespiratory responses of Salmo salar and Squalus acanthias to hyp. *J. Exp. Biol.* **204**, 3963 LP – 3971.

Perry, S. F., Haswell, M. S., Randall, D. J. and Farrell, A. P. (1981). Branchial Ionic Uptake and Acid-Base Regulation in the Rainbow Trout, Salmo Gairdneri. *J. Exp. Biol.* **92**, 289 LP – 303.

Perry, S. F., Fritsche, R., Hoagland, T. M., Duff, D. W. and Olson, K. R. (1999). The control of blood pressure during external hypercapnia in the

948 rainbow trout (Oncorhynchus mykiss). *J. Exp. Biol.* **202**, 2177 LP – 2190.

949 **Pierrot, D., Lewis, E. and Wallace, D. W. R.** (2006). CO2SYS DOS Program
950 developed for CO2 system calculations. *ORNL/CDIAC-105.*

951 **R Core Team** (2020). R: A language and environment for statistical computing.

952 **Roa, J. N., Munévar, C. L. and Tresguerres, M.** (2014). Feeding induces
953 translocation of vacuolar proton ATPase and pendrin to the membrane of
954 leopard shark (Triakis semifasciata) mitochondrion-rich gill cells. *Comp.*
955 *Biochem. Physiol. Part A Mol. Integr. Physiol.* **174**, 29–37.

956 **Rogers, N. J.** (2015). The Respiratory and Gut Physiology of Fish: Response to
957 Environmental Change.

958 **Schindelin, J., Arganda-Carreras, I., Frise, E., Kaynig, V., Longair, M.,**
959 **Pietzsch, T., Preibisch, S., Rueden, C., Saalfeld, S., Schmid, B., et al.**
960 (2012). Fiji: an open-source platform for biological-image analysis. *Nat.*
961 *Methods* **9**, 676–682.

962 **Seo, M. Y., Mekuchi, M., Teranishi, K. and Kaneko, T.** (2013). Expression of
963 ion transporters in gill mitochondrion-rich cells in Japanese eel acclimated
964 to a wide range of environmental salinity. *Comp. Biochem. Physiol. Part A*
965 *Mol. Integr. Physiol.* **166**, 323–332.

966 **Shartau, R. B., Baker, D. W., Harter, T. S., Aboagye, D. L., Allen, P. J., Val,**
967 **A. L., Crossley, D. A., Kohl, Z. F., Hedrick, M. S., Damsgaard, C., et al.**
968 (2020). Preferential intracellular pH regulation is a common trait amongst
969 fishes exposed to high environmental
970 CO{\textless}sub{\textgreater}2{\textless}/sub{\textgreater}. *J. Exp. Biol.*
971 **223**, jeb208868.

972 **Smatresk, N. J. and Cameron, J. N.** (1982). Respiration and Acid-Base
973 Physiology of the Spotted Gar, a Bimodal Breather: II. Responses to
974 Temperature Change and Hypercapnia. *J. Exp. Biol.* **96**, 281 LP – 293.

975 **Sunda, W. G. and Cai, W.-J.** (2012). Eutrophication Induced CO_2-Acidification
976 of Subsurface Coastal Waters: Interactive Effects of Temperature, Salinity,
977 and Atmospheric PCO_2. *Environ. Sci. Technol.* **46**, 10651–10659.

978 **Thomas, S. and Perry, S. F.** (1992). Control and consequences of adrenergic
979 activation of red blood cell Na+/H+ exchange on blood oxygen and carbon
980 dioxide transport in fish. *J. Exp. Zool.* **263**, 160–175.

981 **Toews, D. P., Holeton, G. F. and Heisler, N.** (1983). Regulation of the acid-
982 base status during environmental hypercapnia in the marine teleost fish
983 Conger conger. *J. Exp. Biol.* **107**, 9 LP – 20.

984 **Tovey, K. J. and Brauner, C. J.** (2018). Effects of water ionic composition on
985 acid–base regulation in rainbow trout, during hypercarbia at rest and during
986 sustained exercise. *J. Comp. Physiol. B* **188**, 295–304.

987 **Tresguerres, M. and Hamilton, T. J.** (2017). Acid base physiology,
988 neurobiology and behaviour in relation to CO2-induced ocean acidification.
989 *J. Exp. Biol.* **220**, 2136–2148.

990 **Tresguerres, M., Katoh, F., Fenton, H., Jasinska, E. and Goss, G. G.** (2005).
991 Regulation of branchial V-H+-ATPase, Na+/K+-ATPase and NHE2 in

response to acid and base infusions in the Pacific spiny dogfish (Squalus acanthias). *J. Exp. Biol.* **208**, 345–354.

Tresguerres, M., Parks, S. K., Katoh, F. and Goss, G. G. (2006). Microtubule-dependent relocation of branchial V-H+-ATPase to the basolateral membrane in the Pacific spiny dogfish (Squalus acanthias): a role in base secretion. *J. Exp. Biol.* **209**, 599–609.

Tresguerres, M., Parks, S. K. and Goss, G. G. (2007a). Recovery from blood alkalosis in the Pacific hagfish (Eptatretus stoutii): Involvement of gill V–H+–ATPase and Na+/K+–ATPase. *Comp. Biochem. Physiol. Part A Mol. Integr. Physiol.* **148**, 133–141.

Tresguerres, M., Parks, S. K., Wood, C. M. and Goss, G. G. (2007b). V-H+-ATPase translocation during blood alkalosis in dogfish gills: interaction with carbonic anhydrase and involvement in the postfeeding alkaline tide. *Am. J. Physiol. Integr. Comp. Physiol.* **292**, R2012–R2019.

Tresguerres, M., Milsom, W. K. and Perry, S. F. (2019). 2 - CO2 and acid-base sensing. In *Carbon Dioxide* (ed. Grosell, M.), Munday, P. L.), Farrell, A. P.), and Brauner, C. J. B. T.-F. P.), pp. 33–68. Academic Press.

Verdouw, H., Van Echteld, C. J. A. and Dekkers, E. M. J. (1978). Ammonia determination based on indophenol formation with sodium salicylate. *Water Res.* **12**, 399–402.

Vermette, M. G. and Perry, S. F. (1988). Adrenergic involvement in blood oxygen transport and acid-base balance during hypercapnic acidosis in the Rainbow Trout,Salmo gairdneri. *J. Comp. Physiol. B* **158**, 107–115.

Wallace, R. B., Baumann, H., Grear, J. S., Aller, R. C. and Gobler, C. J. (2014). Coastal ocean acidification: The other eutrophication problem. *Estuar. Coast. Shelf Sci.* **148**, 1–13.

Wells, R. M. G. (2009). Chapter 6 Blood-Gas Transport and Hemoglobin Function: Adaptations for Functional and Environmental Hypoxia. In *Fish Physiology* (ed. Jeffrey G. Richards, A. P. F. and C. J. B.), pp. 255–299. Academic Press.

Wilson, R. W. and Grosell, M. (2003). Intestinal bicarbonate secretion in marine teleost fish—source of bicarbonate, pH sensitivity, and consequences for whole animal acid–base and calcium homeostasis. *Biochim. Biophys. Acta - Biomembr.* **1618**, 163–174.

Wood, C. M., McDonald, D. G. and McMahon, B. R. (1982). The Influence of Experimental Anaemia on Blood Acid-Base Regulation In Vivo and In Vitro in the Starry Flounder (Platichthys Stellatus) and the Rainbow Trout (Salmo Gairdneri). *J. Exp. Biol.* **96**, 221 LP – 237.

Zeidler, R. and Kim, H. D. (1977). Preferential hemolysis of postnatal calf red cells induced by internal alkalinization. *J. Gen. Physiol.* **70**, 385–401.

1. Supplementary materials

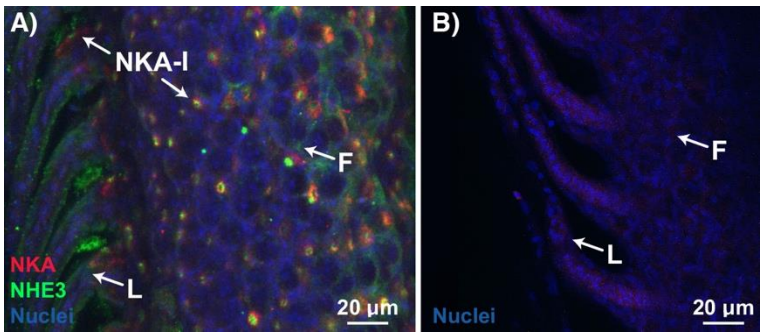

Figure S1: A. Na^+/K^+-ATPase (NKA, red) and Na^+/H^+ Exchanger 3 (NHE3, green) immunostaining within European sea bass gill. Ionocytes containing NKA and NHE3 (NKA-I) were observed on the filament (F) and base of lamellae (L). **B.** Negative controls (no primary antibodies) had no discernible signal. Nuclei (blue) are stained with DAPI.

Table S1: Water chemistry of gill irrigation chambers used while blood sampling fish

	Exposure length			
	0 min	~10 min	~40 min	~135 min
Temperature (°C)	14.00 ± 0.00	14.05 ± 0.15	14.00 ± 0.30	13.95 ± 0.15
pH (NBS)	8.14 ± 0.02	6.95 ± 0.02	6.91 ± 0.01	6.91 ± 0.04
Salinity	34.6 ± 0.4	35.6 ± 0.5	34.8 ± 0.7	34.6 ± 0.7
pCO_2 (µatm)	0.060 ± 0.010	0.965 ± 0.045	1.227 ± 0.164	1.024 ± 0.088
TA (µM)	3120 ± 372	2834 ± 36	3301 ± 361	2750 ± 27

Table S2: Mean ± s.e.m. of water chemistry parameters within isolation tanks during low alkalinity hypercapnia exposure

Duration (min)	**pH (NBS)**	**Temperature (°C)**	**Salinity**	***p*CO₂ (kPa)**	**TA (µM)**
135.0 ± 4.6	5.70 ± 0.03	13.78 ± 0.07	34.0 ± 0.1	1.141 ± 0.020	188 ± 12

Table S3: Water chemistry of gill irrigation chambers used while blood sampling fish in low alkalinity water

pH (NBS)	Temperature (°C)	Salinity	pCO_2 (µatm)	TA (µM)
5.53 ± 0.31	14.05 ± 0.05	35.05 ± 0.25	1.288 ± 0.104	188 ± 129

Table S4: Mean ± s.e.m. of water chemistry parameters within isolation boxes prior to gill sampling. Gill samples from sea bass exposed to hypercapnia were taken from 5 sea bass immediately after flux measurements were completed.

Treatment	Duration (min)	pH (NBS)	Temperature (°C)	Salinity	pCO_2 (kPa)	TA (µM)
Normocapnia	n/a	8.05 ± 0.00	14.12 ± 0.06	33.6 ± 0.0	0.055 ± 0.001	2335 ± 7
Hypercapnia	132.9 ± 2.6	6.97 ± 0.02	14.14 ± 0.02	33.5 ± 0.0	0.770 ± 0.037	2365 ± 9

Table S5: Theoretical calculations of H^+ excretion by NHE in response to environmental hypercapnia. Calculations based on Parks *et al.* 2008. If $Na^+_i/Na^+_e > H^+_i/H^+_e$ then H^+ excretion by NHE is thermodynamically unviable.

Treatment	Ionocyte Na^+ (Na^+_i, mM)	Seawater Na^+ (Na^+_e, mM)	Ionocyte H^+ (H^+_i, mM)	Seawater H^+ (H^+_e, mM)	Na^+_i/Na^+_e	H^+_i/H^+_e
Control	140	480	3.98e^-08	8.91e^-09	0.292	4.467
Hypercapnia	140	480	5.01e^-08	1.12e^-07	0.292	0.447
Hypercapnia + low TA	140	480	5.01e^-08	2.00e^-06	0.292	0.025